Diffusion Tensor Tractography of Traumatic Diffuse Axonal Injury

Jun Yi Wang, MS; Khamid Bakhadirov, MD, MS; Michael D. Devous Sr, PhD; Hervé Abdi, PhD; Roddy McColl, PhD; Carol Moore, MA; Carlos D. Marquez de la Plata, PhD; Kan Ding, MD; Anthony Whittemore, MD, PhD; Evelyn Babcock, PhD; Tiffany Rickbeil, BS; Julia Dobervich, BS; David Kroll, BA; Bao Dao, BS; Nisha Mohindra, BS; Christopher J. Madden, MD; Ramon Diaz-Arrastia, MD, PhD

Background: Diffuse axonal injury is a common consequence of traumatic brain injury that frequently involves the parasagittal white matter, corpus callosum, and brainstem.

Objective: To examine the potential of diffusion tensor tractography in detecting diffuse axonal injury at the acute stage of injury and predicting long-term functional outcome.

Design: Tract-derived fiber variables were analyzed to distinguish patients from control subjects and to determine their relationship to outcome.

Setting: Inpatient traumatic brain injury unit.

Patients: From 2005 to 2006, magnetic resonance images were acquired in 12 patients approximately 7 days after injury and in 12 age- and sex-matched controls.

Main Outcome Measures: Six fiber variables of the corpus callosum, fornix, and peduncular projections were obtained. Glasgow Outcome Scale–Extended scores were assessed approximately 9 months after injury in 11 of the 12 patients.

Results: At least 1 fiber variable of each region showed diffuse axonal injury–associated alterations. At least 1 fiber variable of the anterior body and splenium of the corpus callosum correlated significantly with the Glasgow Outcome Scale–Extended scores. The predicted outcome scores correlated significantly with actual scores in a mixed-effects model.

Conclusion: Diffusion tensor tractography–based quantitative analysis at the acute stage of injury has the potential to serve as a valuable biomarker of diffuse axonal injury and predict long-term outcome.

Arch Neurol. 2008;65(5):619-626

Author Affiliations: Department of Cognition and Neuroscience, The University of Texas at Dallas, Richardson (Ms Wang and Drs Bakhadirov and Abdi); and Departments of Radiology (Drs Devous, McColl, Whittemore, and Babcock, Messrs Kroll and Dao, and Ms Mohindra), Neurology (Mss Moore, Rickbeil, and Dobervich and Drs Marquez de la Plata, Ding, and Diaz-Arrastia), and Neurosurgery (Dr Madden), The University of Texas Southwestern Medical Center at Dallas.

TRAUMATIC BRAIN INJURY (TBI) is a major cause of mortality and disability. In the United States alone, more than 1.4 million cases are reported annually, along with 235 000 hospitalizations and 50 000 deaths.[1] Diffuse axonal injury (DAI) is the predominant mechanism of the injury in 40% to 50% of patients with TBI who require hospitalization[2] and is likely a factor in most cases that result from high-speed motor vehicle collisions. Diffuse axonal injury is a consequence of sustained acceleration and deceleration forces that can shear axons and produce microscopic changes in the brain. In humans, the primary cytoskeleton disorganization can be observed through histologic examinations between 4 and 6 hours after injury. Secondary axotomy normally starts 12 hours after injury,[3] peaks between 1 and 3 days after injury, and may last for years.[4,5] Diffuse axonal injury is a multifocal injury that primarily affects the parasagittal white matter (WM), corpus callosum (CC), and brainstem.[2,3,6]

Fluid attenuation and inversion recovery (FLAIR) imaging can be useful in identifying DAI. It has been reported that FLAIR lesion volume acquired within 2 weeks of the injury correlated moderately with long-term functional outcome as measured by the Glasgow Outcome Scale–Extended (GOSE).[7] Susceptibility-weighted imaging is more sensitive than T2-weighted gradient-echo imaging in detecting hemorrhagic DAI,[8-10] and the quantity and volume of susceptibility-weighted imaging hemorrhages examined at the acute stage of injury correlated well with dichotomized long-term outcome in pediatric patients with TBI.[11] A novel magnetic resonance imaging (MRI) technique, diffusion tensor imaging (DTI), permits the examination of WM integrity in vivo through observing the amount of water diffusion within

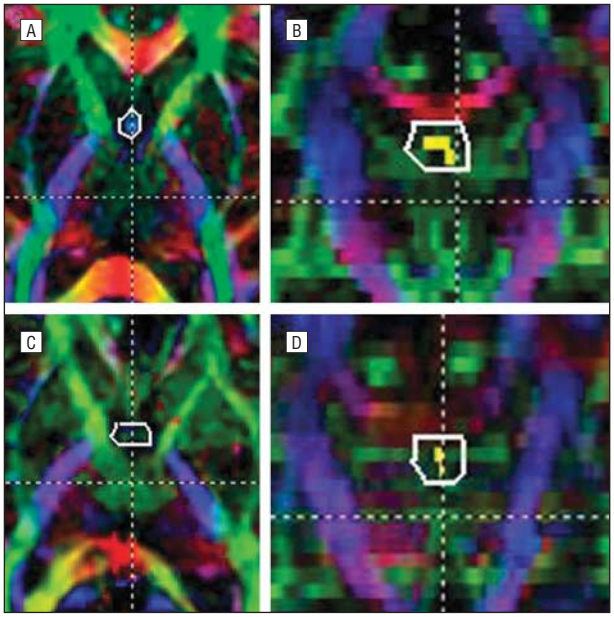

Figure 1. Fornix body reconstruction of a representative control subject (A and B) and a patient (C and D). The first region of interest (ROI) was placed on an axial slice 6 mm superior to the anterior commissure (A and C). The second ROI was placed on the most posterior coronal slice in which the fornix remained as 1 bundle (B and D). The ROI operation used was CUT.

biological tissues.[10,12] A direct comparison between DTI-detected WM integrity changes and histologic findings in an animal model of axonal injury[13] suggests that DTI may become a valuable imaging tool for detecting DAI.

Two diffusion variables have been used[14] for characterizing WM integrity (fractional anisotropy [FA], a ratio of 0 to 1 that represents the degree of alignment of the underlying fibers in a voxel; and mean diffusivity, which represents the presence of overall restrictions to water diffusion). Two studies[15,16] have applied DTI-based region of interest (ROI) analyses in assessing DAI during the acute stage of injury and found loss of structural integrity in the CC, internal and external capsules, and the centrum semiovale. Diffusion tensor tractography (DTT)–based quantification may have advantages over ROI-based DTI analysis.[17] In DTT, the whole length of WM structures of interest can be 3-dimensionally reconstructed through fiber propagation algorithms, and associated fiber measurements can be obtained. A DTT-based quantification has been applied in group analyses in adult[18] and pediatric patients with chronic TBI[19] and has revealed loss of structural integrity in the CC. However, an association between DTI measurements and long-term outcome was only found in patients with chronic TBI using either an ROI-based[20] or a DTT-based[19] approach.

The goals of the present study were to evaluate DTT as a tool for detecting DAI at an early pathologic stage when the injury process was still ongoing and potentially reversible by therapeutic intervention and to identify measures associated with long-term functional outcome. We hypothesized that fiber variables of 3 commonly affected WM tracts (CC, fornix, and peduncular projections [PP]) would correlate better with outcome than standard measures of injury severity and FLAIR-based measurement of WM hyperintensity volume.

Table 1. Patient Demographics

Demographics	Mean (SD)	Median (Range)
Age, y	26 (8.1)	25 (16-37)
GCS score	4.4 (2.1)	3 (3-8)
GOSE score	4.4 (2.2)	4 (1-8)
Time to scan, d	6.7 (4.2)	6.5 (0-15)
Time to follow-up, mo	8.2 (1.6)	9 (6-11)

Abbreviations: GCS, Glasgow Coma Scale; GOSE, Glasgow Outcome Scale–Extended.

METHODS

PATIENTS

From 2005 to 2006, 12 patients with TBI were recruited from Parkland Memorial Hospital, Dallas, Texas. Inclusion criteria required that patients (1) sustained severe closed-head TBIs, (2) had an injury mechanism that was consistent with DAI, (3) had the ability to provide consent or obtain consent from a legal guardian, (4) had at least an eighth-grade education level, and (5) were at least 16 years old. Patients with preexisting neurologic disorders or previous brain injury were excluded from the study. One patient was lost to follow-up. Twelve age- and sex-matched healthy control subjects with good general health and no known neurocognitive disorders were also recruited.

FUNCTIONAL OUTCOME MEASURE

Functional outcomes were determined at least 6 months after injury using the GOSE.[21] The GOSE is a commonly used questionnaire that assesses functional abilities in multiple domains after a head injury and has been shown to be a reliable outcome measure.[22] All outcome interviews and scoring of the GOSE were conducted by 1 of 3 study coordinators (1 of the coordinators was C.J.M.), who were blind to the imaging results. Each rater had at least a bachelor's degree and at least 1 month of experience working with patients with TBI. Each was trained by a neurologist (R.D.-A.) by observing in-person administration of the interview to at least 5 patients and by over-the-telephone administration for 5 patients. A structured questionnaire was used during the follow-up interviews.[21] Each patient was interviewed only once. Interrater reliability for scoring the GOSE was assessed by auditing 20% of the scoring sheets every 3 months. Reproducibility has been greater than 99%. Questionnaires were answered by patients, although in case of death or other severe disability, completion by a caregiver was accepted. Total GOSE scores range from 1 to 8, with higher scores indicating better outcome.

IMAGE ACQUISITION AND PROCESSING

The DTI, T1-weighted, and FLAIR images were acquired by an MRI scanner (GE Signa Excite 3T; General Electric Healthcare, Milwaukee, Wisconsin). The DTI sequences were obtained using a single-shot, spin-echo, echo-planar imaging sequence with a field of view of 240 mm, a slice thickness/gap of 3/0 mm, approximately 45 slices, a repetition time of 12 000 milliseconds, an echo time of 75.5 milliseconds, a flip angle of 90°, number of excitations of 2, and a matrix of 128 × 128. The diffusion-sensitizing gradients were applied at a b value of 1000 s/mm^2 per axis with 19 noncolinear directions and 3 b0 images. The acquisition time was 9 minutes. Voxel size was

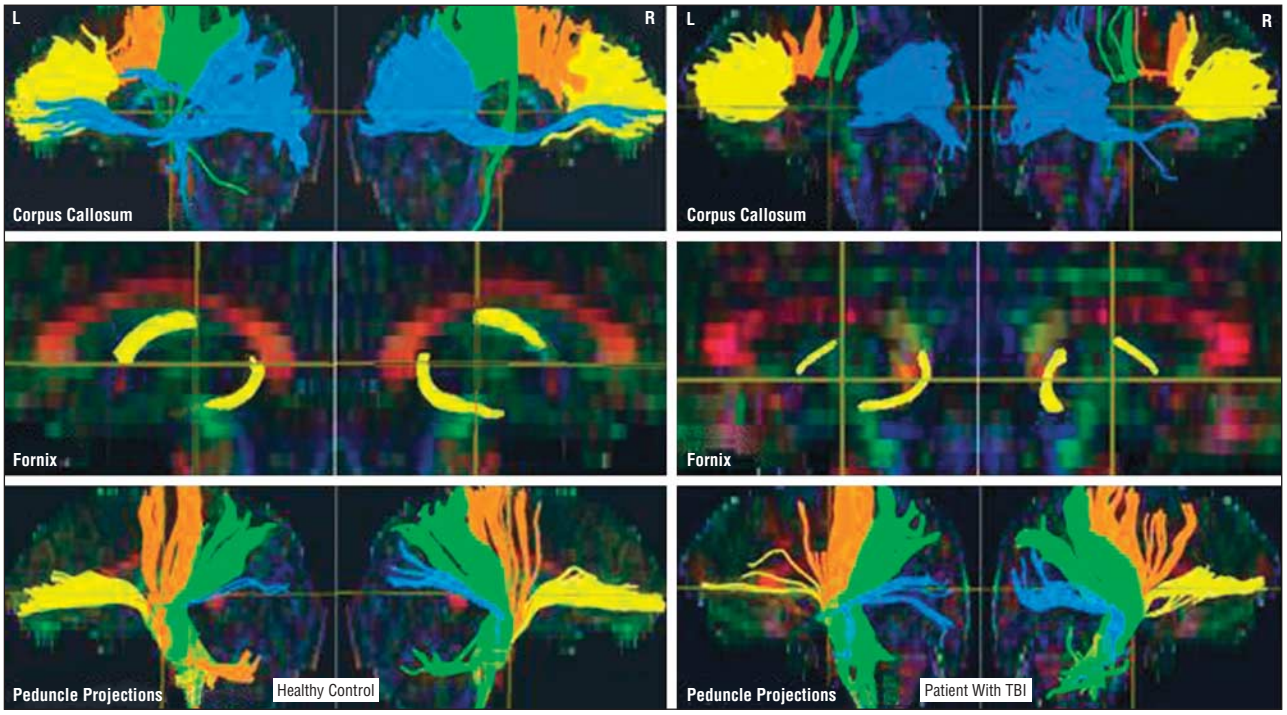

Figure 2. Representative fiber tractography results from a control subject (left) and a patient with traumatic brain injury (TBI) (right). The corpus callosum (top) is parceled into areas 1 through 4 as shown by the corresponding colors yellow, orange, green, or blue. The fornix body and inferior crura are yellow (middle). The peduncular projections (bottom) are parceled into peduncular projections to the ventral frontal cortex (yellow), peduncular projections to the dorsal frontal cortex (orange), peduncular projections to the parietal cortex (green), and peduncular projections to the occipital cortex (blue). The patient did not have cortical contusions on computed tomography, but some shear hemorrhages were noted.

$2 \times 2 \times 3$ mm^3 interpolated (by default at the scanner) to $1 \times 1 \times 3$ mm^3. The T1-weighted structural images were acquired using a fast spoiled gradient-recalled acquisition in the steady state (GRASS) sequence with a field of view of 240 mm, a slice thickness/gap of 1.3/0 mm, approximately 130 slices, an echo time of 2.4 milliseconds, a flip angle of 25°, number of excitations of 2, a matrix of 256×92, and an acquisition time of 6 minutes. The FLAIR images were acquired at the axial plane using tailored radiofrequency and a fast spin-echo sequence with a field of view of 200 to 210 mm, a slice thickness/gap of 3.0/0.5 mm, approximately 28 slices, a repetition time of 9500 milliseconds, an echo time of 136.6 milliseconds, an inversion time of 2500 milliseconds, a flip angle of 90°, an NEX of 1, a matrix of 320×224, and an acquisition time of 4 minutes.

Preprocessing steps for the DTIs included realignment using DTI Studio (Johns Hopkins Medical Institute, http://lbam.med.jhmi.edu/) and brain extraction and eddy-current correction using FSL (http://www.fmrib.ox.ac.uk/fsl/) software applications. Intracranial volumes for normalizing fiber variables were calculated based on T1-weighted structural images using FSL. Diffusion map generation, fiber tractography, and fiber tract quantification were performed in DTI Studio using a fiber tracking FA threshold of 0.25 and an angle threshold of 60°.

IMAGE ANALYSES

Three WM structures susceptible to TBI were included in the analysis.[15,23,24] Fiber tracking adopted a multiple ROI approach[17,25] to increase accuracy and interrater reliability. Anatomical landmarks for ROI slice selections were defined rigorously to reduce subjectivity in fiber tracking. Because CC and PP are large fiber bundles that connect multiple brain regions, they were parceled into sub-tracts for detecting DAI that might affect only a part of the tracts. The CC was parceled into 4 equal areas: CC1 through CC4, corresponding to the genu, anterior and posterior body, and splenium of the CC. The parcellation of PP to ventral frontal, dorsal frontal, parietal, and occipital corticis followed general guidelines of the CC parcellation.[26] The fornix body and left and right crura were tracked separately.[27] **Figure 1** shows representative fornix body ROIs of a control and a patient.

Each WM structure was tracked independently by 2 raters from a pool of 5 (J.Y.W., T.R., J.D., D.K., and B.D.). Fiber variables, including mean FA, tensor trace (total diffusivity or $3 \times$ mean diffusivity), fiber count, mean length, fiber volume, and fiber density index (fiber count per voxel), were recorded. Interrater reliabilities were measured with Pearson product moment correlation coefficients and were greater than 96% for all fiber variables except for those of the fornix crus, which were greater than 87%. Fiber count and fiber volume were normalized using intracranial volume.

FLAIR image analysis followed previously published methods.[7] The WM hyperintensity volumes were estimated using in-house software and normalized with whole brain volume to create a DAI index.

STATISTICAL ANALYSES

We conducted nonparametric rank order analysis to find group differences in the fiber measurements. To find the correlation of GOSE with fiber variables, FLAIR DAI index, and factors such as age, initial Glasgow Coma Scale score, and Trauma Coma Databank computed tomography classification, we performed Spearman rank correlation. The Mann-Whitney test was used to analyze the correlation of GOSE and the categorical variable of sex. $P < .05$ was considered statistically significant, and $P < .005$ was considered statistically significant after correction for multiple comparisons.

To predict GOSE scores from the overall amount of injury in the 3 WM tracts, we first calculated fiber composite indexes using STATIS,[28] a generalization of principal component analysis for

Table 2. Group Comparisons (Patients vs Controls) of Fiber Measurements

Fiber Variable	Controls, Mean (SD)	Patients, Mean (SD)	*P* Value of ROA	Controls, Mean (SD)	Patients, Mean (SD)	*P* Value of ROA
	CC			PVF		
Mean FA	0.59 (0.02)	0.56 (0.02)	<.001[a]	0.52 (0.02)	0.51 (0.02)	.09
Tensor trace, $\mu m^2/ms$	2.18 (0.07)	2.22 (0.12)	.19	2.07 (0.07)	2.20 (0.09)	<.001[a]
Fiber count, $\times 10^3$	12 (1.8)	8.8 (1.6)	<.001[a]	232 (190)	182 (172)	.15
Mean length, mm	94 (5)	89 (6)	.01	114 (14)	107 (12)	.12
Fiber volume, voxels $\times 10^3$	26 (3.8)	21 (3.4)	<.001[a]	2.3 (1.1)	1.8 (1.2)	.11
FDI, fiber count per voxel	43 (3.7)	40 (3.4)	.01	10 (5.4)	8.7 (4.3)	.37
	CC: Genu			PDF		
Mean FA	0.58 (0.02)	0.54 (0.03)	.003[a]	0.55 (0.02)	0.52 (0.04)	.002[a]
Tensor trace, $\mu m^2/ms$	2.20 (0.07)	2.29 (0.19)	.004[a]	2.03 (0.07)	2.12 (0.07)	.002[a]
Fiber count, $\times 10^3$	3.9 (0.6)	3.2 (0.7)	.02	1084 (392)	575 (355)	.002[a]
Mean length, mm	90 (8)	87 (6)	.14	118 (8)	112 (11)	.13
Fiber volume, voxels $\times 10^3$	7.6 (1.2)	6.7 (1.3)	.08	5.2 (1.5)	3.1 (1.4)	.001[a]
FDI, fiber count per voxel	51 (4.8)	46 (5.1)	.01	17 (3.8)	12 (5.0)	.01
	CC: Anterior Body			PPar		
Mean FA	0.54 (0.02)	0.52 (0.04)	.09	0.55 (0.02)	0.52 (0.03)	.002[a]
Tensor trace, $\mu m^2/ms$	2.21 (0.11)	2.22 (0.17)	.50	2.05 (0.07)	2.15 (0.08)	.002[a]
Fiber count, $\times 10^3$	1.3 (0.4)	1.0 (0.4)	.01	713 (440)	500 (426)	.06
Mean length, mm	65 (11)	59 (13)	.08	115 (9)	112 (9)	.17
Fiber volume, voxels $\times 10^3$	3.7 (1.0)	2.7 (1.0)	.0048[a]	4.5 (1.8)	2.9 (1.8)	.02
FDI, fiber count per voxel	21 (4.5)	19 (4.0)	.15	14 (3.3)	13 (5.3)	.41
	CC: Posterior Body			POcc		
Mean FA	0.53 (0.04)	0.49 (0.06)	.02	0.56 (0.02)	0.52 (0.03)	.001[a]
Tensor trace, $\mu m^2/ms$	2.29 (0.17)	2.28 (0.24)	.44	2.12 (0.08)	2.17 (0.08)	.048
Fiber count, $\times 10^3$	1.4 (0.6)	0.9 (0.4)	.01	134 (131)	164 (131)	.18
Mean length, mm	75 (15)	73 (19)	.41	116 (15)	107 (11)	.05
Fiber volume, voxels $\times 10^3$	4.0 (1.4)	2.9 (1.2)	.003[a]	1.7 (1.0)	1.8 (0.8)	.27
FDI, fiber count per voxel	24 (6.2)	21 (6.7)	.11	7.3 (3.5)	8.6 (3.4)	.22
	CC: Splenium			Fornix Body		
Mean FA	0.62 (0.02)	0.57 (0.03)	<.001[a]	0.58 (0.03)	0.52 (0.09)	.01
Tensor trace, $\mu m^2/ms$	2.17 (0.09)	2.17 (0.15)	.31	3.38 (0.31)	3.27 (0.35)	.14
Fiber count, $\times 10^3$	4.8 (0.9)	3.6 (0.6)	<.001[a]	107 (43)	55 (32)	<.001[a]
Mean length, mm	110 (7)	101 (9)	.01	25 (5)	22 (4)	.03
Fiber volume, voxels $\times 10^3$	12.1 (23)	9.1 (1.5)	<.001[a]	172 (44)	120 (39)	<.001[a]
FDI, fiber count per voxel	46 (4.6)	43 (4.4)	.02	16 (4.9)	9.4 (3.8)	.001[a]

Abbreviations: CC, corpus callosum; FA, fractional anisotropy; FDI, fiber density index; GOSE, Glasgow Outcome Scale–Extended; PDF, peduncular projections to the dorsal frontal cortex; PLS, partial least square; POcc, peduncular projections to the occipital cortex; PPar, peduncular projections to the parietal cortex; PVF, peduncular projections to the ventral frontal cortex; ROA, rank order analysis.

[a] $P < .005$.

data compression and integration, and then conducted partial least square (PLS) regression analysis for predicting GOSE scores in a mixed effects model.[29,30] We conducted 2 analyses in a mixed effects model: the fixed and random effects model analyses. The fixed effects model predicted individual GOSE scores based on information from the whole patient group. In the random effects model (or jackknife, $n - 1$ approach), each patient was taken out sequentially and the patient's GOSE score was predicted based on the remaining patients. Finally, the PLS GOSE factor that predicted GOSE best was correlated with the original DTI data to identify fiber variables highly associated with the outcome.

RESULTS

Twelve patients (8 males) with TBI were included in the study. Demographics, injury severity, MRI timing, and outcome assessments are summarized in **Table 1**. Trauma Coma Databank scores were as follows: 1 (normal), 1 patient; 2 (diffuse injury), 10 patients; and 3 (diffuse injury with swell), 1 patient. Follow-up information was not obtained from 1 patient (8%). Although all patients experienced severe TBI as rated by the initial Glasgow Coma Scale score (range, 1-8), the long-term functional outcome was more varied, ranging from good recovery (GOSE score, 8) to death (GOSE score, 1).

The 3-dimensional reconstructions of the CC, fornix, and PP (**Figure 2**) were consistent with those given in previous publications.[25,31] Only fiber variables that showed group differences at $P < .005$ are discussed. At least 1 fiber variable of the whole CC, all subareas of the CC and PP, and the fornix body were significantly different between the patients and controls, with patients showing worse measures ($P < .005$; **Table 2**).

Table 3. Correlation of Fiber Measurements With GOSE and PLS Factor 1

Fiber Variable	Spearman Rank Correlation Coefficient			
	With GOSE	With PLS Factor 1	With GOSE	With PLS Factor 1
	CC		PVF	
Mean FA	0.86[a]	0.92[a]	0.40	0.52
Tensor trace	0.03	0.04	0.17	−0.04
Fiber count	0.80[a]	0.73	0.58	0.77
Mean length	0.52	0.54	0.01	0.09
Fiber volume	0.72	0.52	0.58	0.79[a]
FDI	0.63	0.67	0.57	0.66
	CC: Genu		PDF	
Mean FA	0.30	0.31	0.32	0.41
Tensor trace	−0.51	−0.31	0.41	0.29
Fiber count	0.56	0.49	0.01	−0.14
Mean length	0.17	0.41	0.31	0.36
Fiber volume	0.46	0.31	0.18	0.01
FDI	0.59	0.76	−0.12	−0.21
	CC: Anterior Body		PPar	
Mean FA	0.49	0.57	0.52	0.60
Tensor trace	0.08	0.02	0.21	0.05
Fiber count	0.74	0.81[a]	0.41	0.34
Mean length	0.91[a]	0.93[a]	0.50	0.62
Fiber volume	0.73	0.76	0.38	0.29
FDI	0.84[a]	0.86[a]	0.31	0.20
	CC: Posterior Body		POcc	
Mean FA	0.64	0.66	0.69	0.67
Tensor trace	0.11	0.02	−0.11	−0.10
Fiber count	0.35	0.46	0.59	0.39
Mean length	0.61	0.54	0.73	0.56
Fiber volume	0.37	0.50	0.52	0.31
FDI	0.56	0.55	0.66	0.53
	CC: Splenium		Fornix Body	
Mean FA	0.92[a]	0.86[a]	0.33	0.41
Tensor trace	0.11	0.09	0.13	−0.45
Fiber count	0.53	0.44	−0.01	0.62
Mean length	0.43	0.39	−0.42	0.17
Fiber volume	0.32	0.20	0.17	0.34
FDI	0.71	0.59	0.02	0.66

Abbreviations: CC, corpus callosum; FA, fractional anisotropy; FDI, fiber density index; GOSE, Glasgow Outcome Scale–Extended; PDF, peduncular projections to the dorsal frontal cortex; PLS, partial least square; POcc, peduncular projections to the occipital cortex; PPar, peduncular projections to the parietal cortex; PVF, peduncular projections to the ventral frontal cortex; ROA, rank order analysis.

[a] $P < .005$.

Spearman rank correlation revealed that at least 1 fiber variable of the whole CC, CC2, and CC4 had strong positive correlations with GOSE scores (Spearman $\rho > 0.76$; $P < .005$; **Table 3**). The Spearman rank correlation between PLS regression predicted and actual GOSE scores was 0.91 ($P < .001$) in the fixed effects model and 0.63 ($P = .04$) in the random effects model. Table 3 also gives the Spearman ρ between fiber variables of all WM tracts and the first factor of the PLS regression. In comparison, the 2 statistical methods found primarily similar results, although PLS regression detected more fiber variables that were useful in predicting GOSE scores, including the fiber count of CC2 and the fiber volume of the peduncular projections to the ventral frontal cortex. **Figure 3** shows scatterplots of the mean FA of CC4 (left) and the predicted GOSE scores in the fixed effects (middle) and random effects (right) models against the GOSE scores.

All patients had at least 1 WM hyperintensity on their FLAIR images. The DAI index correlated marginally with the GOSE score (Spearman $\rho = -0.53$, $P = .10$). Age showed a significant correlation with the GOSE score (Spearman $\rho = -0.61$, $P = .046$). Sex, initial Glasgow Coma Scale score, and Trauma Coma Databank scores did not correlate with the outcome in this small sample.

COMMENT

In the present study, we explored techniques to obtain reliable and objective fiber measurements by refining

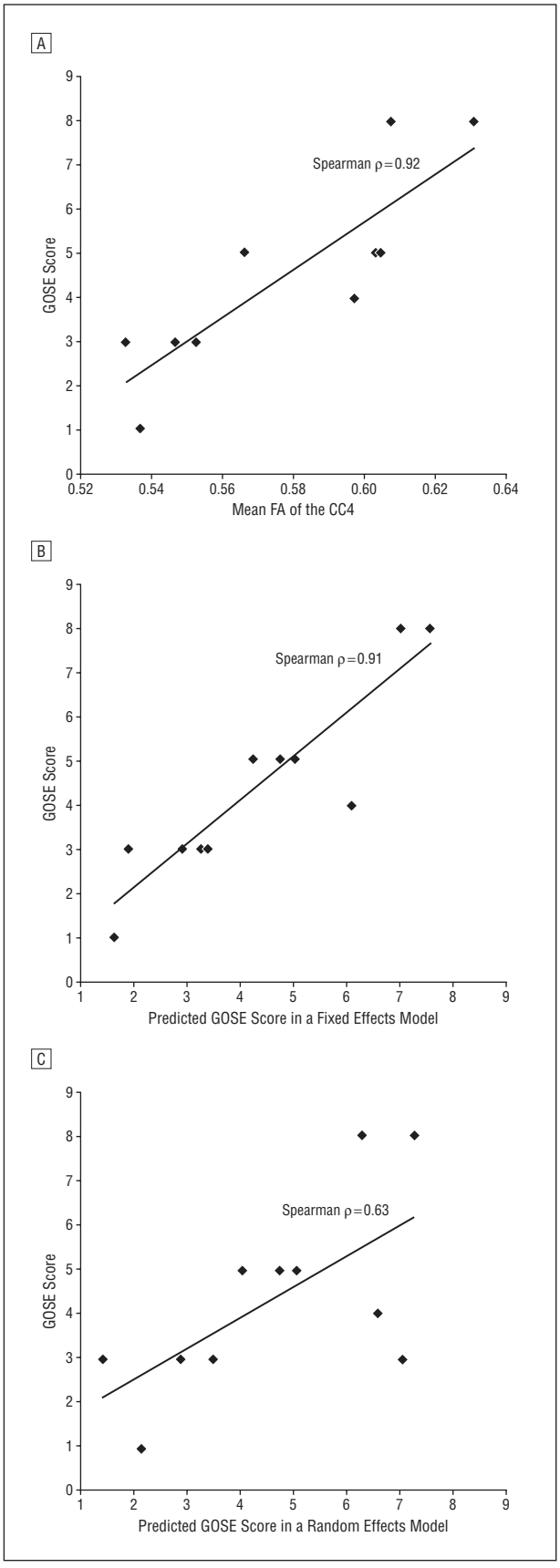

Figure 3. Plots of the mean fractional anisotropy (FA) of corpus callosum area 4 (CC4) (A) and the predicted Glasgow Outcome Scale–Extended (GOSE) scores in fixed effects (B) and random effects (C) models against the GOSE.

fiber-tracking methods. We performed 3-dimensional reconstruction of the CC, fornix, and PP using a multiple-ROI approach to increase interrater reliability.[17,25] To reduce subjectivity in ROI slice selections, we used various anatomical landmarks for finding the image slices. Our interrater reliability has reached 96% and greater for all fiber measurements except for the fornix crus (>89%).

Except for 1 quantitative study[19] in a pediatric population with chronic TBI, previous DTI tractography studies[18,32,33] have concentrated on visualizing fiber trajectory changes associated with TBI. In addition, among DTI studies that used either an ROI or DTI tractography approach, only 1 study of pediatric patients with TBI[19] and 1 study of adult patients with TBI[20] found an association between DTI measures obtained at the chronic stage of injury and outcome. In this pilot study, we tested whether tractography-based quantification of 3 WM structures vulnerable to DAI could detect lesions at an early stage after TBI and whether the tractography variables were associated with long-term outcome. Our results extended previous reports that suggest that DTI might detect loss of WM integrity due to DAI even at the beginning of the injury process and that the DTI measurements at the acute stage of injury were highly associated with long-term functional outcome. We found that at least 1 fiber variable of the fornix body and all subregions of CC and PP were significantly worse in the patient group than the control group. Despite the small sample size (n=11), associations between the DTI measurements and the GOSE scores were robust. Fiber measurements of the whole CC, CC2, and CC4 obtained at the acute stage of injury were highly correlated with the GOSE scores. The correlation between the PLS predicted and actual GOSE scores was 0.91 ($P<.001$) in the fixed effects model and 0.63 ($P=.04$) in the random effects model when incorporating all fiber measurements of the 3 tracts. Moreover, the fiber variables that made significant contribution to the PLS regression corresponded to the fiber variables with significantly high Spearman rank correlation coefficients with the GOSE. **Figure 4** shows the WM regions highly associated with the GOSE.

In comparison, the correlation between the FLAIR DAI index and the GOSE was not statistically significant and was similar to previous findings in a larger data set.[7] Thus, tractography-based quantification may be more useful than FLAIR lesion volume analysis and factors such as age, sex, initial Glasgow Coma Scale score, and Trauma Coma Databank computed tomography classification in prognosis. The correlation between the GOSE score and age was statistically significant (Spearman ρ=−0.61; $P=.046$) but not as strong as the correlation between the GOSE and DTI measurements.

The detection of DAI in the CC, fornix body, and PP is consistent with previous DTI studies. Reduced FA values have been found in the CC, internal and external capsules, and centrum semiovale at the acute stage of injury in mild TBI[15,16] and in the fornix at the chronic stage of injury.[24] The lack of DAI-associated changes in the fornix crura in the present study may be a technical limitation that results from limited DTI image resolution.[27]

Caution must be exercised when interpreting fiber tracking results. The technique is relatively new and the

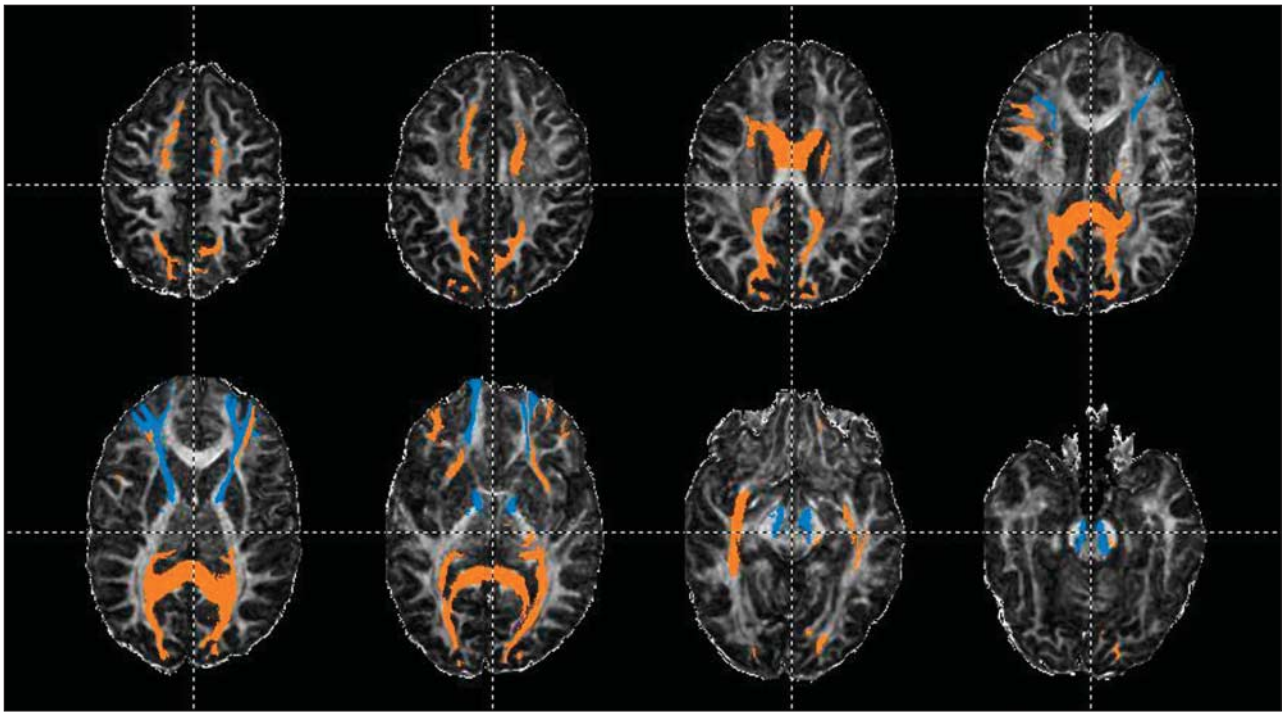

Figure 4. Overlay of fiber tracts highly associated with the Glasgow Outcome Scale–Extended (GOSE) score on a representative fractional anisotropy map of a healthy control. Corpus callosum areas 2 and 4 are orange; peduncular projections to the ventral frontal cortex are blue.

fiber assignment by continuous tracking (FACT) algorithm used in DTI Studio has limitations, particularly in the areas of crossing fibers. Failure or early termination in fiber propagation or fiber jumping onto another tract may exist. The relatively few gradient-encoding directions (n=19) that was state-of-the art when scans were acquired might affect accuracy in tensor calculation. However, our findings suggest that the measurements from these DTI images had an adequate signal-to-noise ratio for DAI diagnosis and prognosis. Other limitations are small sample size and the inclusion of only a subset of WM structures at risk. Investigations to address these limitations are under way.

The present study demonstrated that when implementing carefully designed fiber tracking methods, DTI tractography-based quantification may be useful for detecting DAI and predicting outcome. Our results also indicate that all 6 fiber variables made unique contributions to the analyses.

Accepted for Publication: October 1, 2007.
Correspondence: Ramon Diaz-Arrastia, MD, PhD, Department of Neurology, The University of Texas Southwestern Medical Center at Dallas, 5323 Harry Hines Blvd, Dallas, TX 75390-9063 (ramon.diaz-arrastia@utsouthwestern.edu).
Author Contributions: *Study concept and design:* Wang, Bakhadirov, Abdi, Ding, Whittemore, Kroll, Mohindra, and Diaz-Arrastia. *Acquisition of data:* Wang, Bakhadirov, Devous, McColl, Moore, Marquez de la Plata, Whittemore, Babcock, Rickbeil, Kroll, Dao, and Mohindra, and Madden. *Analysis and interpretation of data:* Wang, Bakhadirov, Devous, Abdi, McColl, Marquez de la Plata, Ding, Whittemore, Dobervich, Kroll, Dao, Mohindra, and Diaz-Arrastia. *Drafting of the manuscript:* Wang, Bakhadirov, Devous, Abdi, Moore, Marquez de la Plata, Ding, Dobervich, and Diaz-Arrastia. *Critical revision of the manuscript for important intellectual content:* Wang, Bakhadirov, Devous, McColl, Marquez de la Plata, Ding, Whittemore, Babcock, Rickbeil, Kroll, Dao, Mohindra, Madden, and Diaz-Arrastia. *Statistical analysis:* Wang, Bakhadirov, Devous, Abdi, Ding, and Diaz-Arrastia. *Obtained funding:* Ding and Diaz-Arrastia. *Administrative, technical, and material support:* Devous, McColl, Moore, Ding, Babcock, Rickbeil, Kroll, Dao, Mohindra, Madden, and Diaz-Arrastia. *Study supervision:* Devous, Marquez de la Plata, Ding, Whittemore, and Diaz-Arrastia.
Financial Disclosure: None reported.
Funding/Support: This study was supported by grant H133 A020526 from the National Institute on Disability and Rehabilitation Research (Dr Diaz-Arrastia) and grants R01 HD48179 and U01 HD42652 from the National Institutes of Health (Dr Diaz-Arrastia).

REFERENCES

1. Langlois JA, Rutland-Brown W, Thomas K. *Traumatic Brain Injury in the United States: Emergency Department Visits, Hospitalizations, and Deaths.* Atlanta, GA: National Center for Injury Prevention and Control; 2006.
2. Meythaler JM, Peduzzi JD, Eleftheriou E, Novack TA. Current concepts: diffuse axonal injury-associated traumatic brain injury. *Arch Phys Med Rehabil.* 2001;82(10):1461-1471.
3. Gaetz M. The neurophysiology of brain injury. *Clin Neurophysiol.* 2004;115(1):4-18.
4. Wilson S, Raghupathi R, Saatman KE, et al. Continued in situ DNA fragmentation of microglia/macrophages in white matter weeks and months after traumatic brain injury. *J Neurotrauma.* 2004;21(3):239-250.
5. Bigler ED. Distinguished Neuropsychologist Award Lecture 1999: the lesion(s) in traumatic brain injury: implications for clinical neuropsychology. *Arch Clin Neuropsychol.* 2001;16(2):95-131.

6. Smith DH, Meaney DF, Shull WH. Diffuse axonal injury in head trauma. *J Head Trauma Rehabil*. 2003;18(4):307-316.
7. Marquez de la Plata C, Ardelean A, Koovakkattu D, et al. Magnetic resonance imaging of diffuse axonal injury: quantitative assessment of white matter lesion volume. *J Neurotrauma*. 2007;24(4):591-598.
8. Scheid R, Walther K, Guthke T, et al. Cognitive sequelae of diffuse axonal injury. *Arch Neurol*. 2006;63(3):418-424.
9. Ashwal S, Babikian T, Gardner-Nichols J, et al. Susceptibility-weighted imaging and proton magnetic resonance spectroscopy in assessment of outcome after pediatric traumatic brain injury. *Arch Phys Med Rehabil*. 2006;87(12)(suppl 2):S50-S58.
10. Metting Z, Rodiger LA, De Keyser J, van der Naalt J. Structural and functional neuroimaging in mild-to-moderate head injury. *Lancet Neurol*. 2007;6(8):699-710.
11. Tong KA, Ashwal S, Holshouser BA, et al. Diffuse axonal injury in children: clinical correlation with hemorrhagic lesions. *Ann Neurol*. 2004;56(1):36-50.
12. Basser PJ, Mattiello J, LeBihan D. Estimation of the effective self-diffusion tensor from the NMR spin echo. *J Magn Reson B*. 1994;103(3):247-254.
13. Mac Donald CL, Dikranian K, Song SK, et al. Detection of traumatic axonal injury with diffusion tensor imaging in a mouse model of traumatic brain injury. *Exp Neurol*. 2007;205(1):116-131.
14. Basser PJ, Pierpaoli C. Microstructural and physiological features of tissues elucidated by quantitative-diffusion-tensor MRI. *J Magn Reson B*. 1996;111(3):209-219.
15. Arfanakis K, Haughton VM, Carew JD, et al. Diffusion tensor MR imaging in diffuse axonal injury. *AJNR Am J Neuroradiol*. 2002;23(5):794-802.
16. Inglese M, Makani S, Johnson G, et al. Diffuse axonal injury in mild traumatic brain injury: a diffusion tensor imaging study. *J Neurosurg*. 2005;103(2):298-303.
17. Mori S, van Zijl PC. Fiber tracking: principles and strategies—a technical review. *NMR Biomed*. 2002;15(7-8):468-480.
18. Xu J, Rasmussen IA, Lagopoulos J, Haberg A. Diffuse axonal injury in severe traumatic brain injury visualized using high-resolution diffusion tensor imaging. *J Neurotrauma*. 2007;24(5):753-765.
19. Wilde EA, Chu Z, Bigler ED, et al. Diffusion tensor imaging in the corpus callosum in children after moderate to severe traumatic brain injury. *J Neurotrauma*. 2006;23(10):1412-1426.
20. Kraus MF, Susmaras T, Caughlin BP, Walker CJ, Sweeney JA, Little DM. White matter integrity and cognition in chronic traumatic brain injury: a diffusion tensor imaging study. *Brain*. 2007;130(pt 10):2508-2519.
21. Wilson JT, Pettigrew LE, Teasdale GM. Structured interviews for the Glasgow Outcome Scale and the Extended Glasgow Outcome Scale: guidelines for their use. *J Neurotrauma*. 1998;15(8):573-585.
22. Hudak AM, Caesar RR, Frol AB, et al. Functional outcome scales in traumatic brain injury: a comparison of the Glasgow Outcome Scale (extended) and the functional status examination. *J Neurotrauma*. 2005;22(11):1319-1326.
23. Huisman TA, Schwamm LH, Schaefer PW, et al. Diffusion tensor imaging as potential biomarker of white matter injury in diffuse axonal injury. *AJNR Am J Neuroradiol*. 2004;25(3):370-376.
24. Nakayama N, Okumura A, Shinoda J, et al. Evidence for white matter disruption in traumatic brain injury without macroscopic lesions. *J Neurol Neurosurg Psychiatry*. 2006;77(7):850-855.
25. Catani M, Howard RJ, Pajevic S, Jones DK. Virtual in vivo interactive dissection of white matter fasciculi in the human brain. *Neuroimage*. 2002;17(1):77-94.
26. Huang H, Zhang J, Jiang H, et al. DTI tractography based parcellation of white matter: application to the mid-sagittal morphology of corpus callosum. *Neuroimage*. 2005;26(1):195-205.
27. Concha L, Gross DW, Beaulieu C. Diffusion tensor tractography of the limbic system. *AJNR Am J Neuroradiol*. 2005;26(9):2267-2274.
28. Abdi H, Valentin D. *STATIS*. Thousand Oaks, CA: SAGE Publications Inc; 2007.
29. McIntosh AR, Lobaugh NJ. Partial least squares analysis of neuroimaging data: applications and advances. *Neuroimage*. 2004;23(suppl 1):S250-S263.
30. Abdi H. *Partial Least Square Regression (PLS Regression)*. Thousand Oaks, CA: SAGE Publications Inc; 2007.
31. Wakana S, Jiang H, Nagae-Poetscher LM, et al. Fiber tract-based atlas of human white matter anatomy. *Radiology*. 2004;230(1):77-87.
32. Naganawa S, Sato C, Ishihra S, et al. Serial evaluation of diffusion tensor brain fiber tracking in a patient with severe diffuse axonal injury. *AJNR Am J Neuroradiol*. 2004;25(9):1553-1556.
33. Le TH, Mukherjee P, Henry RG, Berman JI, Ware M, Manley GT. Diffusion tensor imaging with three-dimensional fiber tractography of traumatic axonal shearing injury: an imaging correlate for the posterior callosal "disconnection" syndrome: case report. *Neurosurgery*. 2005;56(1):189.